VARIATIONS IN PORE STRUCTURE OF ACTIVATED CARBON FIBERS FROM LIQUEFIED WOOD WITH PREOXIDATION TREATMENT

Zhi Jin

PhD Student
E-mail: lucy870828@163.com

*GuangJie Zhao**

Professor
College of Material Science and Technology
Beijing Forestry University
Beijing 100083, China
E-mail: zhaows@bjfu.edu.cn

(Received May 2014)

Abstract. Preoxidation treatments in air at 200-280°C were introduced in the preparation of activated carbon fiber from liquefied wood (LWACF) with steam activation at 910°C to enlarge its pore size distribution (PSD). LWACF yield was improved 1.14 times with preoxidation at 200°C. With increasing preoxidation temperature, the specific surface area increased from 2592 to 3068 m^2/g. Preoxidations at 200 and 240°C predominantly enhanced the microporosity development without significant pore widening, whereas preoxidation at 280°C significantly enlarged the PSD. Mesopore volume increased by 72%, and methylene blue adsorption capacity improved by 34%.

Keywords: Preoxidation, liquefied wood, activated carbon fiber, pore development, mesoporosity.

INTRODUCTION

Activated carbon fiber (ACF) has been widely used as an adsorbent for purification and pollution control (Gupta et al 2010), catalyst supports (Huang et al 2008), polarizable electrodes (Xu et al 2010), and gas storage (Im et al 2009) because of its large specific surface area and pore volume as well as high adsorption–desorption rate. In general, ACF is commercially produced from raw materials such as coal tar pitch, polyacrylonitrile, viscose rayon, and phenol resin with relatively high burnoff (70-80%). To ease petrochemical resource shortages, it is necessary to develop low-cost raw materials and enhance the production efficiency of ACF. Recently, ACF from liquefied wood (LWACF) was developed. Like in commercial petrochemical-based ACF, it possesses a micropore-dominated structure (Liu and Zhao 2012; Jin and Zhao 2014). However, ACF with a larger pore size (mesopores) is needed because it allows absorption of large amounts (Ozaki et al 1997) and sizes of molecules and is superior in some applications, eg electrode materials (Xu et al 2010) and hydrogen storage (Konwar and De 2013). Researchers have shown that additives, such as polymer (Ozaki et al 1997), catalyst (Oya et al 1995), or nonmetal additives (carbon black or wood charcoal) (Zhang et al 1997; Ma et al 2014), added to the carbon source can lead to pore size distribution (PSD) enlargement in ACF.

Preoxidation treatment (air preoxidation of precursors at 200-300°C) plays an important role in enhancing porosity development of activated carbon (AC) by formation of oxygen groups, which increases the number of active sites (Fdez Ferreras et al 1993; Karimi et al 2013). Parra et al (1996) prepared AC from semianthracite preoxidized at 270°C. The resulting AC possessed higher amounts of both small and medium microporosity than those without oxidation pretreatment. Seggiani et al (2005) revealed that the mesopore volume of AC from heavy-oil fly ash was enhanced by 0.597 cm^3/g with preoxidation at 250°C for 36 h. Liu et al (2010) showed that

* Corresponding author

the mesopore percentage of phenolic-resin-based AC increased from 51.2 to 92.3% with preoxidation at 300°C for 120 min.

Thus, preoxidation treatment has the potential to enlarge the PSD in ACF. It is also thought to be simply operated and can effectively avoid the use of costly polymer or catalyst, as well as the fiber fracture during spinning and ionic impurity caused by the addition of additives. In this study, preoxidations in air at 200-280°C for 60 min are introduced in the preparation of LWACF, and the effect of preoxidation temperature on its porosity development was studied.

MATERIALS AND METHODS

Sample Preparation

Dried Chinese fir (*Cunninghamia lanceolata* [Lamb.] Hook.) flour passing 40-60 mesh was mixed with phenol (wood/phenol = 1/6 by weight) containing 8 wt% phosphoric acid as a reaction catalyst. The mixture was liquefied in a 500-mL three-neck glass flask at 160°C for 2.5 h with continuous stirring. The resulting liquefied wood was synthesized at 175°C for 20 min with 5 wt% hexamethylenetetramine and spun at 120-130°C. The resultant fiber was cured by soaking in an acid solution of formaldehyde and hydrochloric acid (37:30 by volume) at 90°C for 2 h at a rate of 15°C/h, washed with deionized water, and finally dried at 85°C for 2 h to gain liquefied wood precursor fiber (LWPF). The LWPF was oxidized at constant temperatures of 200, 240, and 280°C for 60 min at a rate of 0.5°C/min in air with a flow of 0.6 m^3/h to prepare liquefied wood preoxidized fiber (LWPOF). LWPF and LWPOF were heated up to 910°C at a rate of 4°C/min in a nitrogen stream and then activated at 910°C for 60 min by introducing steam mixed with N_2 stream. The samples were abbreviated to "abbreviation preoxidation temperature."

Elemental Analysis

An A FLASH EA1112 Elemental Analyzer (ThermoFisher Scientific, Waltham, MA) was used for elemental analysis of LWPF and LWPOF.

Fourier Transform Infrared Spectroscopy Analysis

Fourier transform infrared (FTIR) spectra of LWPF and LWPOF were measured on a Brukert Tensor 27 spectrometer (Brukert Optics, Bejing, China) using the KBr disk method. The fibers were pulverized to 150-200 mesh and mixed with KBr before being pressed into a disk. The KBr concentration of the sample was 2.5%, and 0.2 g of KBr was used in the preparation of the reference and sample disks.

Scanning Electron Microscopy Analysis

Scanning electron microscopy (SEM) (Hitachi S-3400N Variable Pressure SEM, Tokyo, Japan) was used for the surface morphology observations of LWPF, LWPOF, and LWACF.

Yield Analysis

Preoxidation yield (Y_P), activation yield (Y_A), and total yield (Y) of LWACF were calculated, respectively, as follows:

$$Y_P = w_1 / w_0 \times 100\% \quad (1)$$

$$Y_A = w_2 / w_1 \times 100\% \quad (2)$$

$$Y = Y_P \times Y_A \times 100\% \quad (3)$$

where w_0 and w_1 were the weight of the fiber before and after preoxidation, respectively, and w_2 was the weight of the fiber after activation.

Pore Characterization

Pore features of LWACF were obtained from the nitrogen adsorption–desorption at –196°C by an adsorption apparatus (Autosorb-iQ; Quantachrome Instruments, Boynton Beach, FL). Before each measurement, LWACF was degassed at 300°C for 3 h. Specific surface area (S_{BET}) and average pore size (D_a) were calculated

by Brunauer-Emmett-Teller surface area measurement. Micropore specific surface area (S_{mi}) was obtained by the t-plot method. Total pore volume (V_t) was based on the nitrogen volume adsorbed at the highest relative pressure. Micropore volume (V_{mi}), mesopore volume (V_{me}), and PSD were determined by density functional theory.

Methylene Blue Adsorption Test

The methylene blue (MB) adsorption test followed GB/T 12496.10-1999 (Chinese National Standard 1999).

RESULTS AND DISCUSSION

Characterization of Liquefied Wood Precursor Fiber and Liquefied Wood Preoxidized Fiber

Elemental analysis. Changes of element contents of LWPF and LWPOF with preoxidation temperature are plotted in Fig 1. As can be seen, oxygen content and ratio of oxygen to carbon increased, whereas carbon and hydrogen content decreased with increasing preoxidation temperature. These results clearly show that preoxidation allowed formation of oxygen functional groups by consuming hydrocarbon functional groups.

Fourier transform infrared analysis. Figure 2 shows FTIR spectra of LWPF and LWPOF. Significant changes occurred in the regions listed in Table 1. The relative intensities of peaks at 3000-3600 cm^{-1}, 1450 cm^{-1}, 2854 cm^{-1}, and 2915 cm^{-1} progressively decreased with increasing preoxidation temperature, and the relative intensities of peaks at 1650-1900 cm^{-1} obviously increased after preoxidation. It was found that the preoxidation treatment formed C=O functional groups through consuming aliphatic C-H and OH groups. This result is similar to the result presented in Worasuwannarak et al (2003), which shows that the aliphatic groups were selectively oxidized to form the ketones first and then further oxidized to form the carboxyls and the quinones as well as the esters as the preoxidation time was prolonged from 0 to 60 min at 220-270°C. In this study, the absorbance values of peaks at ketones (1650 cm^{-1}), quinones (1680 cm^{-1}), carboxyls

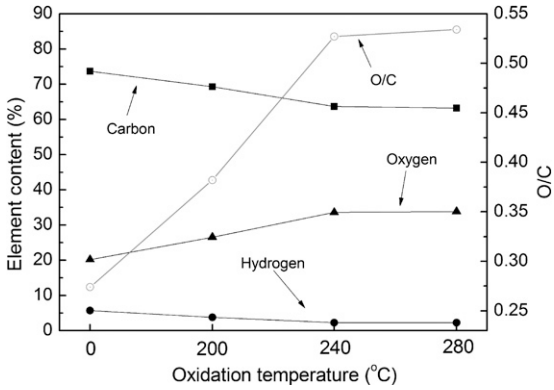

Figure 1. Changes of element contents with preoxidation temperature.

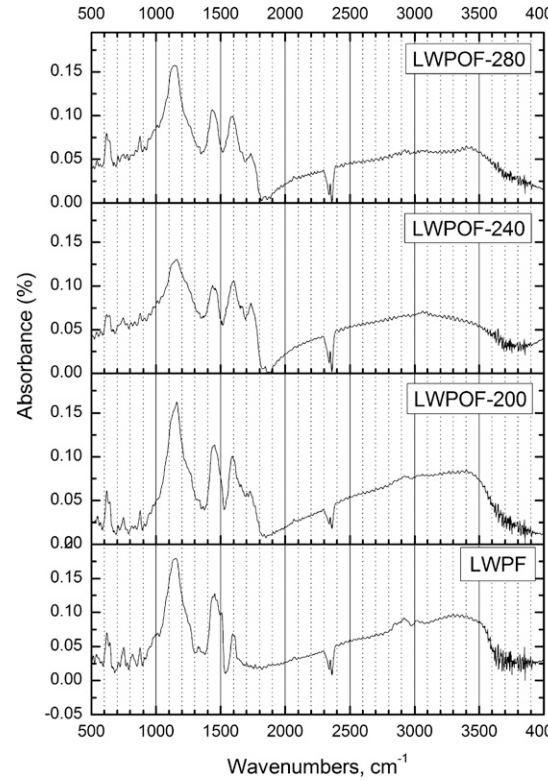

Figure 2. Fourier transform infrared spectra of liquefied wood precursor fiber (LWPF) and liquefied wood preoxidized fiber (LWPOF).

Table 1. Fourier transform infrared spectroscopy peak assignments for liquefied wood precursor fiber and liquefied wood preoxidized fiber.

Wavenumber (cm^{-1})	Assignments
760, 820, 870, 3020	Aromatic C-H adsorption bands (Jung et al 2001; Worasuwannarak et al 2003)
1150	C-O stretching vibration of ether (including cyclic ether containing C-O-C-O-C groups), alcoholic, phenolic, and carboxylic groups (Stein et al 2009; Shen et al 2011)
1450, 2854, 2915	Aliphatic C-H adsorption bands (Jung et al 2001; Worasuwannarak et al 2003)
1516, 1600	Out-of-plane twisting or wagging of aromatic skeleton and aromatic C=C stretching vibration (Braun et al 2005)
1650-1900	C=O stretching (Jung et al 2001; Yoshida et al 2005)
3000-3600	O-H stretching region (Kodama et al 1992)

(1720 cm^{-1}), and esters (1740 cm^{-1}) reached maximums at 240°C and then decreased at 280°C, indicating that less C=O groups were formed at 280°C. Meanwhile, the relative intensity of the peak at 1150 cm^{-1} significantly decreased to a minimum at 240°C and then increased at 280°C, suggesting that the preoxidation also consumed C-O groups at 200 and 240°C, whereas some new C-O groups were formed at 280°C. Besides, a small amount of new hydrogen bonds was formed at 280°C, which can be evidenced by peaks at 3460-3580 cm^{-1} and 3250-3400 cm^{-1} with slightly stronger relative intensity than those at 240°C. Conversely, the relative intensities of peaks at 760 cm^{-1}, 820 cm^{-1}, 870 cm^{-1}, 1516 cm^{-1}, and 1600 cm^{-1} significantly increased with rising preoxidation temperature to 240°C and then remained consistent at 280°C, implying aromatic ring condensation was accomplished at 240°C. Thus, it is inferred that the pendant groups of aromatic rings were almost volatilized and replayed by C-O groups and hydrogen bonds to connect aromatic rings when preoxidized at 280°C.

Scanning electron microscopic analysis. SEM images of LWPF and LWPOF (Fig 3) show that the diameter of LWPF decreased with increasing preoxidation temperature. This decrease in diameter is in accordance with the decrease in Y_P (Table 2), which was probably caused by the volatilization of hydrocarbon functional groups and the condensation of aromatic rings. Furthermore, crevices and holes only occurred on the surface of LWPOF-280. This might be attributed to decarboxylation reactions as well as the reconnection of aromatic rings at 280°C. As mentioned in the study on preoxidation effects on the pore structure of phenolic resin-based activated carbon spheres, the smooth surface of the precursor influences the penetration of activated reagent and prevents the development of porous texture of the activated sample (Liu et al 2010). Therefore, crevices and holes on LWPOF-280 would promote the pore formation of LWACF during the activation process.

Characterization of Activated Carbon Fiber from Liquefied Wood

Yield analysis. As shown in Table 2, the Y_A of activated LWPOF was higher than that of activated LWPF and increased to a maximum by preoxidation at 240°C. Previous literature has demonstrated that the oxygen combined by preoxidation can lead to formation of larger amounts of CO and CO_2 during carbonization allowing the tar to be suppressed. Consequently, the yield of ACF was improved (Worasuwannarak et al 2002, 2003). Finally, LWACF with preoxidation at 200°C maximized Y, which was 1.14 times higher than that of activated LWPF.

Scanning electron microscopic analysis. In Fig 4a-d, we can see that the surface characteristic of LWACF displays a clear morphological variation with the series of the preoxidation process. As the preoxidation temperature increased, LWACF began to show more pores on its surface and a wider distribution. Furthermore, the fiber diameter of LWACF-280 was significantly smaller than those of other activated samples, coincident with its lowest value of Y. Thus, in

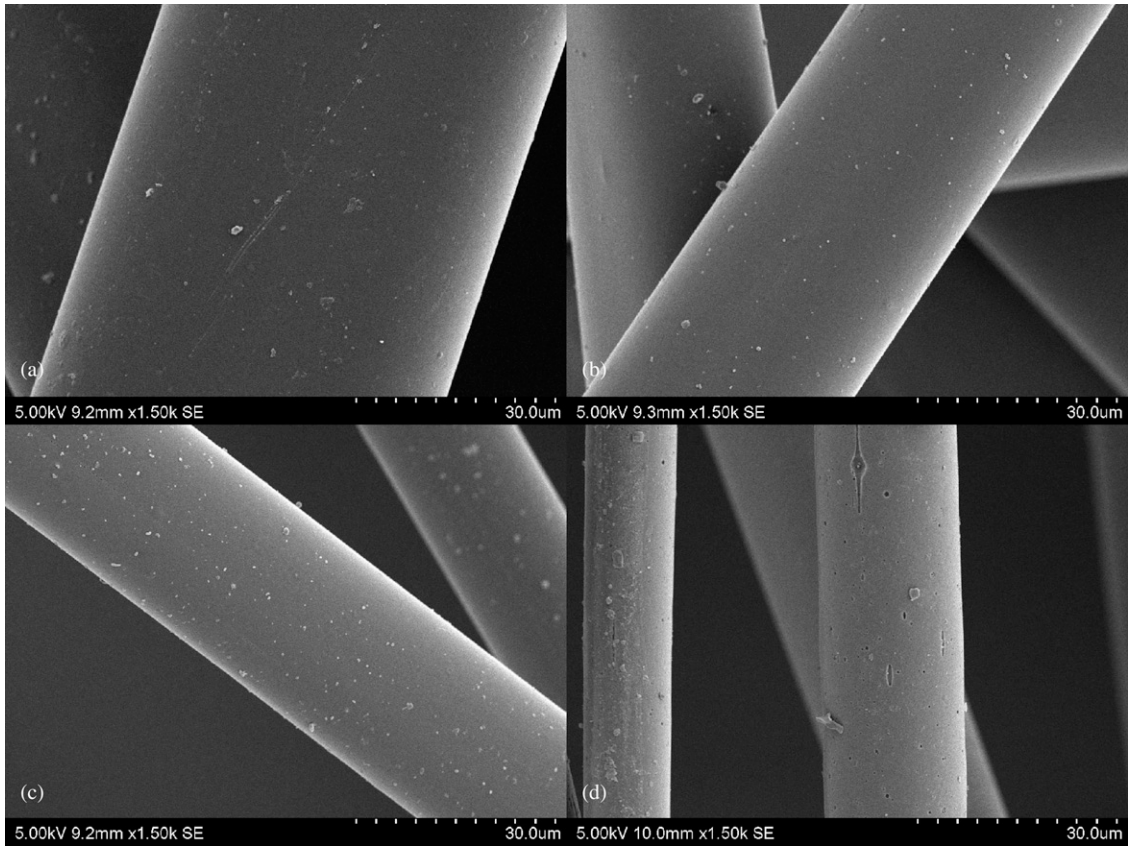

Figure 3. Scanning electron microscope images of precursor fibers (a) liquefied wood precursor fiber; (b) liquefied wood preoxidized fiber (LWPOF)-200; (c) LWPOF-240; and (d) LWPOF-280.

Table 2. Preoxidation yield, activation yield, and total yield of the prepared samples.[a]

	Y_P (%)	Y_A (%)	Y (%)
LWPF	100.0	—	—
LWPOF-200	96.6	—	—
LWPOF-240	77.1	—	—
LWPOF-280	40.1	—	—
LWACF	—	12.4	12.4
LWACF-200	—	14.6	14.1
LWACF-240	—	15.6	12.0
LWACF-280	—	13.4	5.4

[a] LWPF, liquefied wood precursor fiber; LWPOF, liquefied wood preoxidized fiber; LWACF, liquefied wood activated carbon fiber.

parallel with the promotion in pore development, preoxidation at 280°C accelerated the fiber surface erosion during activation.

Pore structural analysis. Figure 5a-b shows the nitrogen isotherms of LWACF at –196°C. All the isotherms were type I (IUPAC classification) showing a highly microporous nature. Also, the isotherm of LWACF-280 exhibited a widening knee and a longer hysteresis (Fig 5b) suggesting the domination of mesoporosity. Maximum nitrogen adsorption volume increased from 849 to 1117 cm^3/g with increasing preoxidation temperature.

The porosity parameters derived from the nitrogen isotherms are reported in Table 3. It clearly shows that preoxidation played an important role in promoting the pore formation in LWACF. S_{BET} and V_t were enhanced by 6.5, 11.0, and 18.4% and by 8.6, 12.4, and 31.6%, respectively, with increasing preoxidation temperature. Such phenomenon is possibly caused by the fact that the increase of oxygen functional groups formed in the LWPF leads to more

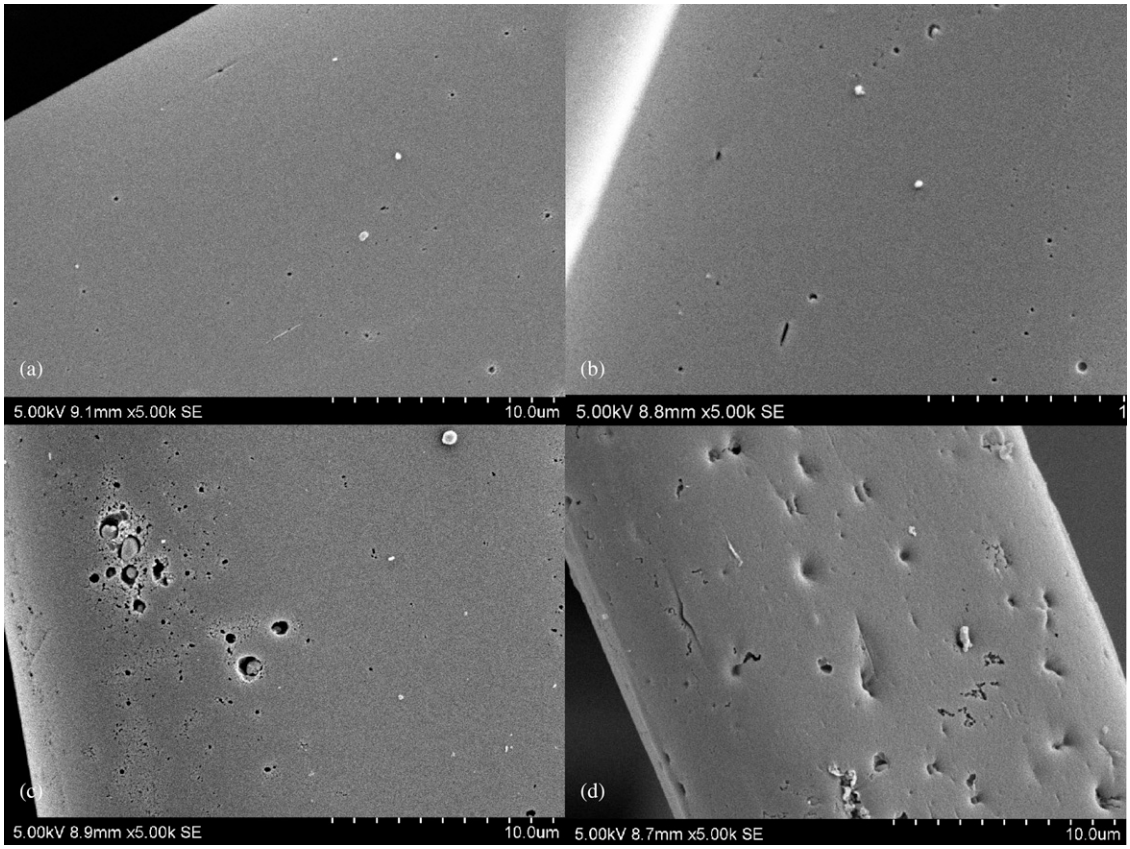

Figure 4. Scanning electron microscope images of activated fibers (a) liquefied wood activated carbon fiber (LWACF); (b) LWACF-200; (c) LWACF-240; and (d) LWACF-280.

efficient removal of the volatiles during the carbonization process and further helps in the enlargement in the primary porous structure of the carbonized fiber (PPS-CF), which allows deep penetration of activated reagent for activation to create more pores (He 2004).

Also, preoxidation at 200 and 240°C considerably increased the microporosity. As the preoxidation temperature increased from 200 to 240°C, both S_{mi} and V_{mi} continuously increased and attained maximum by preoxidation at 240°C. However, D_a was almost kept unchanged, which suggests that preoxidation at these two temperatures did not have significant effects on the pore size enlargement of LWACF. Comparatively, preoxidation at 280°C significantly promoted the development of mesoporosity rather than microporosity. The V_{me} and mesopore percentage were improved by 72 and 12%, respectively, which gives rise to the increase of the D_a from 2.03 to 2.25 nm. Correspondingly, S_{mi} decreased from 2089 to 1929 m^2/g. Thus, for LWACF-280, the mesoporosity appeared to develop from the micropores, possibly in the way that mesopores are formed by collapse and coalescence of the micropores. Meanwhile, the extremely high S_{BET} (3068 m^2/g) and V_t (1.728 cm^3/g) in LWACF-280 was completely attributed to the remarkable mesoporosity development.

All this agrees well with the observation in the PSD of LWACF (Fig 5c-d). Compared with LWACF-200 and LWACF-240, LWACF-280 presented remarkable augmentations in the amount of larger micropores (1.3-1.8 nm) and mesopores (2.4-6.0 nm), showing that pore development took place mainly by pore widening by

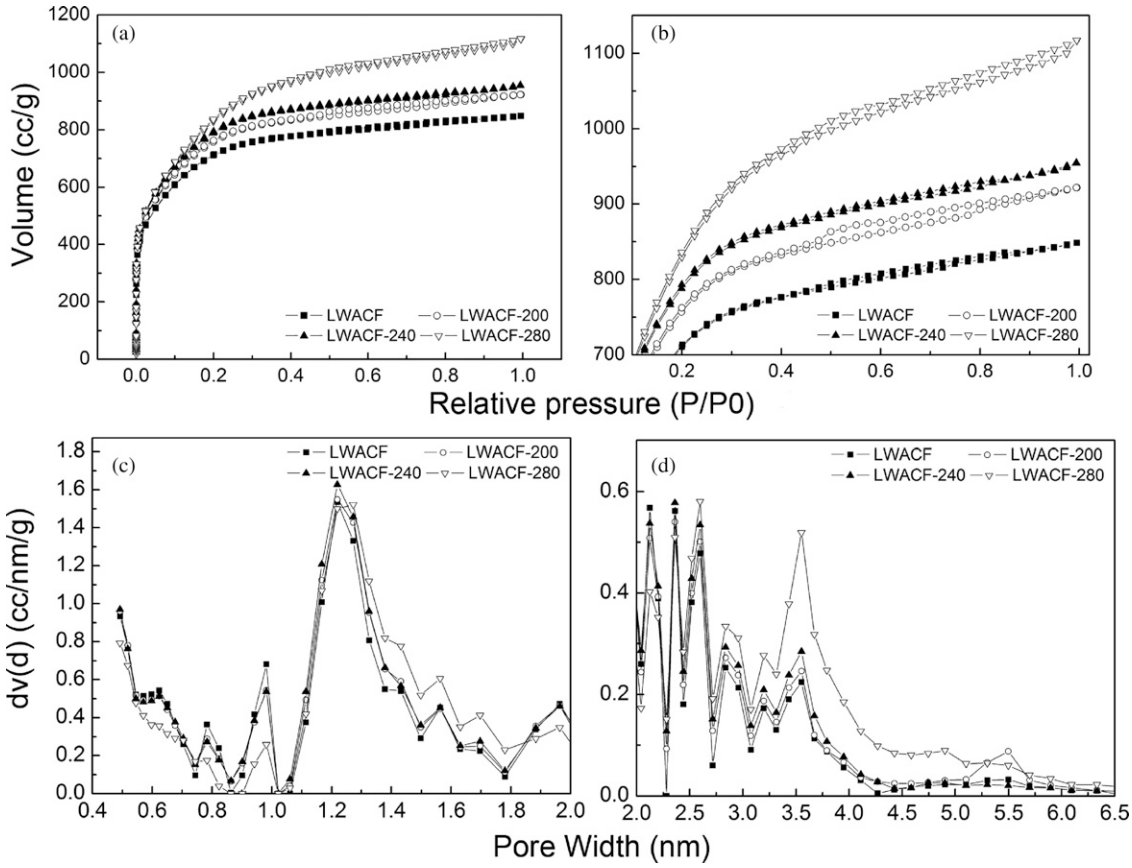

Figure 5. (a) Nitrogen adsorption–desorption isotherms at –196°C of the obtained liquefied wood activated carbon fiber (LWACF); (b) partial enlargements of Fig 3a; (c) pore size distribution (PSD) of LWACF in the micropore region; and (d) PSD of LWACF in the mesopores region.

Table 3. Pore characteristics and adsorption capacity for methylene blue (MB) of liquefied wood activated carbon fiber (LWACF).

	Pore structure parameters							Adsorption test
Samples	S_{BET} (m^2/g)	S_{mi} (m^2/g)	V_t (cm^3/g)	V_{mi} (cm^3/g)	V_{me} (cm^3/g)	V_{me}/V_t (%)	D_a (nm)	MB (mg/g)
LWACF	2592	2089	1.313	0.747	0.514	39	2.03	458
LWACF-200	2760	2187	1.426	0.786	0.585	41	2.06	488
LWACF-240	2877	2310	1.476	0.804	0.610	41	2.05	503
LWACF-280	3068	1929	1.728	0.769	0.885	51	2.25	615

preoxidation at 280°C. This significant enlargement in the PSD might be explained by the crevices and holes on the surface of LWPOF-280 (Fig 3d), which could promote the development of PPS-CF. Conversely, the microporosity development by preoxidations at 200 and 240°C is judged to occur mainly through pore drilling, ie formation of new micropores or deepening of the existing micropores without significant pore widening (Karimi et al 2013).

Methylene blue adsorption. To investigate the large molecule adsorption of LWACF with preoxidation, the MB decolorization test was

carried out. The MB adsorption capacity increased with the rise of preoxidation temperature, which roughly corresponded to the development of mesoporosity (Table 3). With the greatest mesopore volume (0.885 cm^3/g), LWACF-280 exhibited the highest MB adsorption value of 615 mg/g.

CONCLUSIONS

The porosity of LWACF was better developed with increasing preoxidation temperature, possibly because of the increasing oxygen functional groups formed in the precursor fiber, which might lead to the enlargement in the PPS-CF. Especially, preoxidations at 200 and 240°C predominantly enhanced the microporosity development by pore drilling, whereas preoxidation at 280°C significantly enlarged the pore size distribution with the mesopore volume increased by 72% and MB adsorption capacity improved by 34%. This effect appears to be closely related to the crevices and holes on the surface of the precursor fiber caused by the decarboxylation reactions and reconnection of aromatic rings when preoxidized at 280°C, which could promote the development of PPS-CF.

ACKNOWLEDGMENTS

We are grateful for the support of the Specialized Research Fund for the Doctoral Program of Higher Education, Grant. No. 20130014130001.

REFERENCES

Braun JL, Holtman KM, Kadla JF (2005) Lignin-based carbon fibers: Oxidative thermostabilization of kraft lignin. Carbon 43(2):385-394.

Chinese National Standard (1999) GB/T 12496.10-1999. Test methods of wooden activated carbon—Determination of methylene blue adsorption. Chinese National Standard, Beijing, China.

Fdez Ferreras J, Blanco C, Pajares JA, Mahamud M, Pis JJ (1993) A combined FTIR and textural study of the pre-oxidation of a bituminous coal. Spectrosc Lett 5(26):897-912.

Gupta AK, Deva D, Sharma A, Verma N (2010) Fe-grown carbon nanofibers for removal of arsenic(V) in wastewater. Ind Eng Chem Res 49(15):7074-7084.

He F (2004) Carbon fiber and its application technology. Chemical Industry Press, Beijing, China. 180 pp.

Huang HX, Chen SX, Yuan C (2008) Effect of calcination temperature on activity of Cu-ACF catalysts in catalytic wet oxidation of ammonia solution. J Power Sources 175(1):166-174.

Im JS, Jung MJ, Lee YS (2009) Effects of fluorination modification on pore size controlled electrospun activated carbon fibers for high capacity methane storage. J Colloid Interface Sci 339(1):31-35.

Jin Z, Zhao G (2014) Porosity evolution of activated carbon fiber prepared from liquefied wood. Part I: Water steam activation at 650 to 800°C. Bioresources 9(2):2237-2247.

Jung MW, Ahn KH, Lee Y, Kim KP, Rhee JS, Park JT, Paeng KJ (2001) Adsorption characteristics of phenol and chlorophenols on granular activated carbons (GAC). Microchem J 70(2):123-131.

Karimi A, Thinon O, Fournie J, Hill JM (2013) Activated carbon prepared from Canadian oil sands coke by CO_2 activation: I. Trends in pore development and the effect of pre-oxidation. Can J Chem Eng 91(9):1491-1499.

Kodama M, Fujiura T, Esumi K, Meguro K, Honda H (1992) Carbonization and graphitization of meso-carbon microbeads prepared by the emulsion method. J Mater Sci 27(22):6079-6085.

Konwar RJ, De M (2013) Effects of synthesis parameters on zeolite templated carbon for hydrogen storage application. Microporous Mesoporous Mater 175(15):16-24.

Liu Y, Li KX, Sun GH (2010) Effect of precursor preoxidation on the structure of phenolic resin-based activated carbon spheres. J Phys Chem Solids 71(4):453-456.

Liu W, Zhao G (2012) Effect of temperature and time on microstructure and surface functional groups of activated carbon fibers prepared from liquefied wood. Bioresources 7(4):5552-5567.

Ma XJ, Zhang F, Zhu JY, Yu LL, Liu XY (2014) Preparation of highly developed mesoporous activated carbon fiber from liquefied wood using wood charcoal as additive and its adsorption of methylene blue from solution. Biores Technol 164:1-6.

Oya A, Yoshida S, Alcaniz-monge J, Linares-Solano A (1995) Formation of mesopores in phenolic resin-derived carbon fiber by catalytic activation using cobalt. Carbon 33(8):1085-1090.

Ozaki J, Endo N, Ohizumi W, Igarashi K, Nakahara M, Oya A (1997) Novel preparation method for the production of mesoporous carbon fiber from a polymer blend. Carbon 35(7):1031-1033.

Parra JB, Pis JJ, Desousa JC, Pajares JA, Bansal RC (1996) Effect of coal preoxidation on the development of microporosity in activated carbons. Carbon 34(6): 783-787.

Seggiani M, Vitolo S, Filippis PD (2005) Effect of preoxidation on the porosity development in a heavy oil fly ash by CO_2 activation. Fuel 84(12-13):1593-1596.

Shen Q, Zhang T, Zhang WX, Chen S, Mezgebe M (2011) Lignin-based activated carbon fibers and controllable

pore size and properties. J Appl Polym Sci 121(2): 989-994.

Stein A, Wang Z, Fierke MA (2009) Functionalization of porous carbon materials with designed pore architecture. Adv Mater 21(3):265-293.

Worasuwannarak N, Hatori S, Nakagawa H, Miura K (2003) Effect of oxidation pre-treatment at 220 to 270°C on the carbonization and activation behavior of phenolic resin fiber. Carbon 41(5):933-944.

Worasuwannarak N, Nakagawa H, Miura K (2002) Effect of pre-oxidation at low temperature on the carbonization behavior of coal. Fuel 81(11-12):1477-1484.

Xu B, Wu F, Chen RJ, Cao GP, Chen S, Yang YS (2010) Mesoporous activated carbon fiber as electrode material for high-performance electrochemical double layer capacitors with ionic liquid electrolyte. J Power Sources 195(7):2118-2124.

Yoshida C, Okabe K, Yao T, Shiraishi N, Oya A (2005) Preparation of carbon fibers from biomass-based phenol–formaldehyde resin. J Mater Sci 40(2): 335-339.

Zhang YZ, Wang MZ, He F, Zhang BJ (1997) Mesopore development in PAN–ACF resulting from non-metal additives. J Mater Sci 32(22):6009-6013.